THE ASTROPHYSICAL JOURNAL, 634:L13–L16, 2005 November 20

HCN $J = 5$–4 EMISSION IN APM 08279+5255 AT $z = 3.91$[1]

J. WAGG,[2,3] D. J. WILNER,[2] R. NERI,[4] D. DOWNES,[4] AND T. WIKLIND[5]
Received 2005 October 4; accepted 2005 October 14; published 2005 November 2

ABSTRACT

We detect HCN $J = 5$–4 emission from the ultraluminous quasar APM 08279+5255 at $z = 3.911$ using the IRAM Plateau de Bure Interferometer. This object is strongly gravitationally lensed, yet still thought to be one of the most intrinsically luminous objects in the universe. The new data imply a line luminosity $L'_{\mathrm{HCN}(J=5-4)} = (4.0 \pm 0.5) \times 10^{10}$ K km s^{-1} pc^2. The ∼440 km s^{-1} FWHM of the HCN $J = 5$–4 line matches that of the previously observed high-J CO lines in this object and suggests that the emission from both species emerges from the same region: a warm, dense circumnuclear disk. Simple radiative transfer models suggest an enhanced abundance of HCN relative to CO in the nuclear region of APM 08279+5255, perhaps due to increased ionization, or possibly the selective depletion of oxygen. The ratio of far-infrared luminosity to HCN luminosity is at the high end of the range found for nearby star-forming galaxies, but is comparable to that observed in the few high-redshift objects detected in the HCN $J = 1$–0 line. This is the first clear detection of high-J HCN emission redshifted into the 3 mm atmospheric window.

Subject headings: galaxies: active — galaxies: high-redshift — galaxies: ISM — quasars: emission lines — quasars: individual (APM 08279+5255)

1. INTRODUCTION

The quasar APM 08279+5255, serendipitously discovered by Irwin et al. (1998), has become an archetypical ultraluminous high-redshift source for study at all wavelengths, from X-ray to radio (e.g., Ellison et al. 1999; Gallagher et al. 2002; Soifer et al. 2004). The popularity of this source may be attributed in part to its tremendous apparent luminosity, of which $\sim 10^{15}\ L_\odot$ emerges in the far-infrared (Lewis et al. 1998). Optical imaging reveals multiple source components and suggests that the object is strongly gravitationally lensed (Ledoux et al. 1998; Ibata et al. 1999; Egami et al. 2000). Even after correction for the lensing amplification, APM 08279+5255 remains one of the most intrinsically luminous objects known in the universe.

The extreme luminosity of APM 08279+5255 is provided by a combination of an active galactic nucleus (AGN) and star formation activity. Downes et al. (1999, hereafter D99) used the IRAM Plateau de Bure Interferometer (PdBI) to detect dust continuum and CO $J = 4$–3 and $J = 9$–8 emission at arcsecond scales in APM 08279+5255, proposing that the emission originates in a warm, dense circumnuclear disk of sub-kpc size. APM 08279+5255 is the only high-redshift source in which CO emission from such highly excited levels as $J = 9$ has been observed, indicative of extreme conditions in the molecular gas. In order to better understand the excitation of the molecular material and its physical nature, observations of additional diagnostic lines are needed.

The HCN molecule, which requires substantially higher densities ($n_{\mathrm{H}_2} > 10^4$ cm^{-3}) than CO for collisional excitation, due to its large dipole moment,t is a promising tracer of environments such as the nucleus of APM 08279+5255. In the Galaxy, HCN emission selectively traces the high-density gas where star formation takes place (Helfer & Blitz 1997). In nearby star-forming galaxies, the HCN $J = 1$–0 line luminosity is found to closely correlate with infrared/far-infrared luminosity (Solomon et al. 1992a; Gao & Solomon 2004a, 2004b). At high redshifts, detection of HCN emission has proven challenging for the current generation of radio telescopes. The $J = 1$–0 line has been clearly detected in H1413+117 (the strongly lensed "Cloverleaf" at $z = 2.6$; Solomon et al. 2003) and in the strongly lensed IRAS F10214+4724 at $z = 2.3$ (Vanden Bout et al. 2004), and tentatively detected in J1409+5628 at $z = 2.6$ (Carilli et al. 2005). The higher excitation HCN $J = 4$–3 line was also tentatively detected in H1413+117 (Barvainis et al. 1997; although see Solomon et al. 2003). Here we present the detection of strong HCN $J = 5$–4 line emission in APM 08279+5255 at $z = 3.9$ and discuss the implications for the physical conditions in this remarkable object.

We adopt the following Λ-dominated cosmological parameters: $H_0 = 70$ km s^{-1} Mpc^{-1}, $\Omega_\Lambda = 0.7$, and $\Omega_m = 0.3$ (Spergel et al. 2003).

2. OBSERVATIONS

The IRAM PdBI was used to observe APM 08279+5255 in the HCN $J = 5$–4 line, redshifted to the 3 mm band, on six dates in 1999 and 2001. All of the observations were made in compact configurations of the four or five available antennas. The phase center was offset by 1″.25 from the CO peak position. The receivers were tuned to 90.229 GHz, corresponding to the HCN $J = 5$–4 line (rest frequency of 443.1162 GHz) at $z = 3.911$, determined from the earlier CO line observations. Spectral correlators covered a velocity range of ∼1600 km s^{-1}. The baseline lengths ranged from 17 to 81 m, leading to a beam size of 7″.4 × 6″.2 (position angle 79°). The nearby quasar 0749+540 was used for complex gain calibration. The flux scale was set using standard sources and other strong sources including MWC 349, CRL 618, 3C 345.3, and 0923+392, and should be accurate to better than 20%. The integration time on

[1] Based on observations carried out with the IRAM Plateau de Bure Interferometer. IRAM is supported by INSU/CNRS (France), MPG (Germany), and IGN (Spain).

[2] Harvard-Smithsonian Center for Astrophysics, Cambridge, MA 02138; jwagg@cfa.harvard.edu.

[3] Instituto Nacional de Astrofísica, Óptica y Electrónica (INAOE), Apartado Postal 51 y 216, Puebla, Mexico.

[4] Institut de Radio Astronomie Millimétrique, Saint Martin d'Hères, F-38406, France.

[5] ESA Space Telescope Division, STScI, 3700 San Martin Drive, Baltimore, MD 21218.

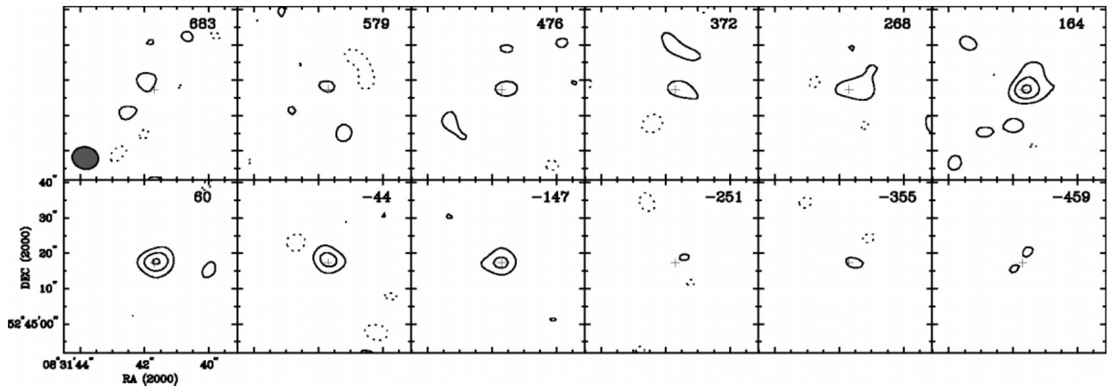

FIG. 1.—Channel maps of 90.2 GHz redshifted HCN $J = 5$–4 emission, plus continuum emission in APM 08279+5255. The cross marks the position of the CO peak position from D99, offset by (1".19, −0".36) from the phase center (08h31m41.s57, 52°45m17.s7). The contour intervals are −2, 2, 4, and 6 σ (0.47 mJy beam^{-1}). The filled ellipse shows the 7".4 × 6".2, P.A. = 79°.0 synthesized beam. The numbers in each panel indicate the velocity relative to $z = 3.911$.

source was about 32 hr (equivalent to 11.9 hr with the current six-antenna array). The average rms noise is 0.47 mJy beam^{-1} in each 100 km s^{-1} channel.

3. RESULTS

Figure 1 shows a series of 100 km s^{-1} channel maps across ∼900 km s^{-1} of the bandwidth. Compact HCN $J = 5$–4 line emission is clearly evident. Figure 2 shows the spectrum at the position of peak intensity in Figure 1. This position is consistent with that found by D99 for the CO emission within the uncertainties. The bandwidth is barely adequate to span the full extent of the HCN line emission. As indicated in Figure 2, we adopt narrow continuum regions at both ends of the spectrum to derive the HCN line properties. The 90.2 GHz continuum flux from the combination of these "line-free" spectral regions is 0.66 ± 0.18 mJy, in line with the value of 1.2 ± 0.3 mJy at 93.9 GHz found by D99, within the uncertainties. A Gaussian fit to the continuum-subtracted spectrum gives a peak flux of 2.01 ± 0.51 mJy beam^{-1}, central velocity $v_0 = 83 \pm 26$ km s^{-1} ($z = 3.9124 \pm 0.0004$), and $\Delta V_{\rm FWHM} = 440 \pm 59$ km s^{-1}. The HCN $J = 5$–4 line integrated intensity determined by integrating over the velocity range −200 to +500 km s^{-1} is 0.98 ± 0.12 Jy km s^{-1}. The line luminosity is $L'_{\rm HCN(J=5-4)} = (4.0 \pm 0.5) \times 10^{10}$ K km s^{-1} pc^2 using equation (3) of Solomon et al. (1992b). Table 1 lists the fitted and derived HCN line parameters.

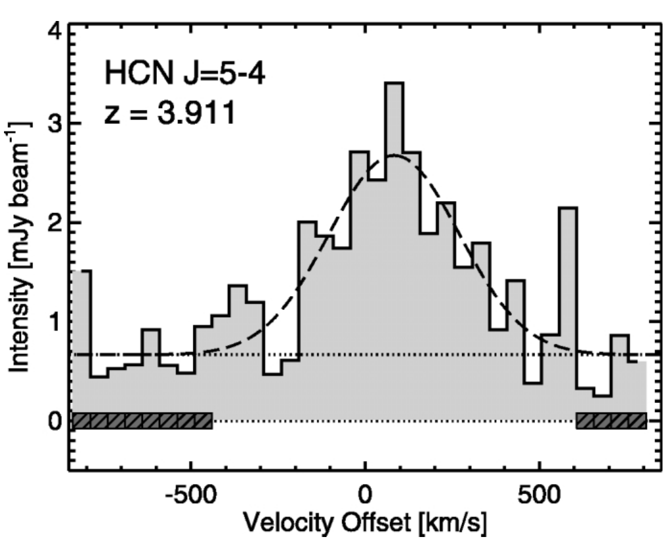

FIG. 2.—Spectrum of HCN $J = 5$–4 emission from APM 08279+5255 at 90.229 GHz, where the velocity scale is relative to the CO redshift of 3.911. The hatched regions mark the channels assumed to represent the line-free continuum level. The dashed line shows a Gaussian fit.

4. DISCUSSION

4.1. *HCN and CO Emission Region*

The HCN $J = 5$–4 central velocity and line width, $\Delta V_{\rm FWHM} = 440 \pm 59$ km s^{-1}, are very similar to that found for the CO $J = 4$–3 line, $\Delta V_{\rm FWHM} = 480 \pm 35$ km s^{-1} (D99). This close correspondence suggests a cospatial origin for the emission from these lines. Both species likely arise from the same dynamical structure, presumably a warm, dense circumnuclear disk.

If the high-J HCN and high-J CO lines emerge from the same region, then it is reasonable to assume that the HCN luminosity is magnified by gravitational lensing by the same factor as the CO luminosity. D99 argue that the magnification factor is 7 to 20 for an intrinsic CO source size of 160–270 pc (173–290 pc for the cosmology adopted here). Lewis et al. (2002) argue for a somewhat lower magnification factor of ∼3, based on the brightness of CO $J = 1$–0 and 2–1 lines in subarcsecond resolution VLA images (Papadopoulos et al. 2001; Lewis et al. 2002). Since the low-J CO line shapes are not well measured, it is not clear if the low-J and high-J CO lines are cospatial. In any case, there is considerable uncertainty in the lensing model, and a wide range of magnification factors are viable. Observations that spatially resolve the high-J CO line emission would be useful to directly probe the line brightness and distribution.

TABLE 1
HCN $J = 5$–4 LINE PARAMETERS FOR APM 08279+5255

Parameter	Value
HCN $J = 5$–4 peak	2.01 ± 0.51 mJy
HCN $J = 5$–4 $\Delta V_{\rm FWHM}$	440 ± 59 km s^{-1}
HCN $J = 5$–4 v_0[a]	83 ± 26 km s^{-1}
$I_{\rm HCN(J=5-4)}$	0.98 ± 0.12 Jy km s^{-1}
$L'_{\rm HCN(J=5-4)}$[b]	(4.0 ± 0.5) × 10^{10} K km s^{-1} pc^2
90.2 GHz continuum	0.66 ± 0.18 mJy

[a] Velocity with respect to $z = 3.911$, determined from the CO lines.

[b] The HCN $J = 5$–4 luminosity is uncorrected for lensing magnification.

4.2. HCN/CO *Ratio and Physical Conditions*

The L' ratio for two lines equals the intrinsic brightness temperature ratio averaged over the velocity and physical extent of the source, and can be used to constrain the physical conditions of the gas (Solomon et al. 1992b). D99 reproduce the CO $J = 9$–$8/J = 4$–3 line luminosity ratio of 0.48 ± 0.07 using escape-probability radiative transfer, and deduce a gas temperature $T_{\rm kin} \sim 140$–250 K and a molecular hydrogen density $n_{\rm H_2} \sim 4000\ {\rm cm^{-3}}$. The CO $J = 9$–$8/J = 4$–3 ratio and the CO $J = 4$–$3/J = 1$–0 ratio can also be reproduced by gas with a lower temperature and higher density. Using the RADEX[6] (Schöier et al. 2005) software, we find that $T_{\rm kin} \sim 80$ K and $n_{\rm H_2} \sim 40{,}000\ {\rm cm^{-3}}$ matches the CO line ratios, with $N({\rm CO})/\Delta v = 4 \times 10^{17}\ {\rm cm^{-2}}\ ({\rm km\ s^{-1}})^{-1}$. This single-component model also provides a good fit to all the observed lines in the CO ladder, up to the $J = 11$–10 transition, as shown by A. Weiss et al. (2005, in preparation), who reach similar conclusions about the gas density and temperature.

These radiative transfer calculations assume that the HCN molecules are excited by collisions. It is possible that radiative excitation plays a role, as infrared radiation from dust heated by the AGN may excite HCN through stretching and bending vibrational modes at (rest frame) 3, 5, and 14 μm. However, as argued by D99 for CO excitation in this source, the large dust mass and consequent high opacity likely prohibits the short-wavelength infrared radiation from affecting a large volume of the gas.

If we assume the conditions inferred from the CO line ratios, and a nominal [HCN/CO] abundance ratio of 10^{-3}, as found in Galactic star-forming cores (Helfer & Blitz 1997), then the single-component radiative transfer model predicts a magnified luminosity $L'_{{\rm HCN}(J=5-4)} = 3.9 \times 10^{9}$ K km s^{-1} pc^{2}, which is a factor of 10 lower than the observed value. A plausible way to produce a higher HCN $J = 5$–4 line luminosity is with a higher [HCN/CO] abundance ratio. From the radiative transfer model, this ratio must be in the range $(1$–$2) \times 10^{-2}$ to match the data. There are at least two plausible scenarios that could lead to a higher [HCN/CO] abundance ratio: (1) an increased ionization rate in the vicinity of the AGN that enhances the HCN abundance (Lepp & Dalgarno 1996), or (2) selective depletion of oxygen relative to carbon in the nuclear region. A combination of these two effects has been proposed to explain observations of HCN and CO in the nearby active nucleus NGC 1068 (Sternberg et al. 1994; Shalabiea & Greenberg 1996; Usero et al. 2004). If there has been selective depletion of oxygen in APM 08279+5255, then the supersolar Fe-to-O ratio found from X-ray data (Hasinger et al. 2002) may not provide a relevant constraint on metal enrichment (or age) at high redshift.

Observations of additional HCN transitions would allow the physical conditions of the HCN-emitting material to be determined independently of the constraints provided by CO observations. The single-component model (with enhanced $[{\rm HCN/CO}] = 10^{-2}$) predicts $L'_{{\rm HCN}(J=1-0)} = 4.4 \times 10^{10}$ K km s^{-1} pc^{2}. A secure detection of the HCN $J = 1$–0 line at this luminosity (redshifted to 18.05 GHz) would require ∼100 hr of integration time using a 100 m diameter class radio telescope.

The mass of dense gas can be estimated from the HCN line luminosity $M_{\rm dense} = \alpha L'_{{\rm HCN}(J=1-0)}$, where α, for warm gas (∼50 K), is ∼7 $M_\odot$ (K km s^{-1} pc^{2})$^{-1}$ (Gao & Solomon 2004b). For the HCN $J = 1$–0 line luminosity estimated from our radiative transfer calculation, $M_{\rm dense} = (3.1 \pm 0.4) \times 10^{11}\ M_\odot$, uncorrected for amplification by gravitational lensing. A conventional estimate of the (total) molecular gas mass from the nuclear CO line luminosity (Lewis et al. 2002) results in a comparable value; i.e., $M_{\rm H_2} = \beta L'_{{\rm CO}(1-0)}$, where $\beta \sim 1$–$5\ M_\odot$ (K km s^{-1} pc^{2})$^{-1}$ (Downes & Solomon 1998; Young & Scoville 1991). In this regard, APM 08279+5255 is somewhat similar to IRAS F10214+4724, where the molecular medium is also dense.

4.3. *Far-Infrared,* CO, *and* HCN *Luminosities*

According to Solomon et al. (2003), the presence of strong HCN emission from a high-redshift object is an indicator of an ongoing starburst. A close correlation exists between far-infrared luminosity and HCN $J = 1$–0 line luminosity in star-forming galaxies (Solomon et al. 1992a). The far-infrared luminosity is primarily due to dust heated by young, high-mass stars. To the extent that AGN activity is not important, the ratio $L_{\rm FIR}/L'_{\rm CO}$ measures the star formation rate per unit of molecular gas mass, while the ratio $L_{\rm FIR}/L'_{\rm HCN}$ measures the star formation rate per unit of dense molecular gas. For the sample of star-forming galaxies examined by Gao & Solomon (2004a, 2004b), $L_{\rm FIR}/L'_{\rm CO}$ increases with far-infrared luminosity, while $L_{\rm FIR}/L'_{\rm HCN}$ does not.

To examine APM 08279+5255 in the context of the correlations established from nearby galaxies, we must appeal to the results of the radiative transfer calculation (§ 4.2) to predict the HCN $J = 1$–0 line luminosity, since this line was not observed. For galaxies in the local universe, generally only the HCN $J = 1$–0 line has been observed; the higher frequency HCN $J = 5$–4 line is not accessible to ground-based observations, due to a strong water absorption feature in the Earth's atmosphere.

Observed values of $L_{\rm FIR}/L'_{\rm HCN}$ for star-forming galaxies are typically less than 2000 $L_\odot$ (K km s^{-1} pc^{2})$^{-1}$. The high-redshift objects with secure HCN $J = 1$–0 detections are H1413+117, F10214+4724, and J1409+5628 and show $L_{\rm FIR}/L'_{\rm HCN}$ of 1700, 3000, and 5000, respectively (Carilli et al. 2005). For APM 08279+5255, the spectrum has been decomposed into starburst and AGN components by Rowan-Robinson (2000), who concludes $L_{\rm FIR} = 9.9 \times 10^{13}\ L_\odot$ (under our assumed cosmology) from the starburst. Adopting this value, $L_{\rm FIR}/L'_{\rm HCN} = 2300$, similar to the ratios observed in the other high-redshift objects and at the high end of the ratios observed in local galaxies. This ratio is sensitive to the detailed decomposition of the spectrum and would be higher if a higher fraction of $L_{\rm FIR}$ were due to star formation rather than AGN activity. This calculation also does not account for the possible effects of differential lensing, and it is plausible that differential lensing results in a higher magnification factor for the far-infrared emission than for the HCN emission, since the molecular gas may have a larger spatial extent (D99), and that could lead to an enhanced apparent value.

Perhaps the nearest analog to APM 08279+5255 in the local universe is Mrk 231, an ultraluminous infrared galaxy with an AGN, whose bolometric luminosity is dominated by a starburst (Solomon et al. 1992a; Davies et al. 2004). In Mrk 231, $L'_{\rm HCN}/L'_{\rm CO} \sim 0.25$, the highest in the Gao & Solomon (2004a) sample. In APM 08279+5255, $L'_{\rm HCN}/L'_{\rm CO} = 0.34 \pm 0.09$, using the (inferred) HCN $J = 1$–0 luminosity and the (observed) nuclear CO $J = 1$–0 luminosity (Papadopoulos et al. 2001). This is at the high end of the range 0.10–0.25 found for local galaxies (Gao & Solomon 2004a, 2004b). The fact that both

[6] See http://www.strw.leidenuniv.nl/~moldata/radex.html.

Mrk 231 and APM 08279+5255 exhibit high $L'_{\rm HCN}/L'_{\rm CO}$ values suggests a possible connection between the presence of an AGN and a high, dense gas mass fraction. A physical mechanism to explain this connection might be that radiation pressure leads to an increased gas density in the vicinity of the AGN, as has been suggested for H1413+117 (Barvainis et al. 1997).

5. SUMMARY

We have detected HCN $J = 5$–4 emission from the ultraluminous quasar APM 08279+5255 at $z = 3.91$. The similarity of the HCN $J = 5$–4 line profile to the CO $J = 4$–3 and $J = 9$–8 lines suggests the emission from these species is cospatial. We have used a simple radiative transfer model to constrain the physical conditions in the molecular gas. The warm ($T_{\rm kin} \sim 80$ K), dense ($n_{\rm H_2} \sim 40{,}000$ cm^{-3}) gas is presumably located in a circumnuclear disk. However, the [HCN/CO] abundance ratio appears to be enhanced.

This is the first clear detection of high-J HCN emission redshifted into the 3 mm atmospheric window. Such observations of high-J transitions of dense gas tracers are expected to become routine with the Atacama Large Millimeter Array, which will provide an improvement in sensitivity by more than an order of magnitude. Observations of dense gas tracers in large samples of high-redshift ultraluminous galaxies will help to probe their power sources, as well as star formation/AGN activity.

6. ACKNOWLEDGMENTS

We thank the IRAM PdBI staff for carrying out these observations. J. W. thanks the SAO for support through a predoctoral student fellowship and the Department of Astrophysics at INAOE for a graduate student scholarship. This work was partially supported by CONACYT grant 39953-F. We thank Floris van der Tak for helpful discussions about radiative transfer, and the RADEX team for making their software available. We are grateful to the anonymous referee for promptly providing helpful suggestions and comments.

REFERENCES

Barvainis, R., Maloney, P., Antonucci, R., & Alloin, D. 1997, ApJ, 484, 695
Carilli, C. L., et al. 2005, ApJ, 618, 586
Davies, R. I., Tacconi, L. J., & Genzel, R. 2004, ApJ, 613, 781
Downes, D., Neri, R., Wiklind, T., Wilner, D. J., & Shaver, P. A. 1999, ApJ, 513, L1 (D99)
Downes, D., & Solomon, P. M. 1998, ApJ, 507, 615
Egami, E., Neugebauer, G., Soifer, B. T., Matthews, K., Ressler, M., Becklin, E. E., Murphy, T. W., & Dale, D. A. 2000, ApJ, 535, 561
Ellison, S. L., Lewis, G. F., Pettini M., Sargent, W. L. W., Chaffee, F. H., Foltz, C. B., Rauch, M., & Irwin, M. J. 1999, PASP, 111, 946
Gallagher, S. C., Brandt, W. N., Chartas, G., & Garmire, G. P. 2002, ApJ, 567, 37
Gao, Y., & Solomon, P. M. 2004a, ApJS, 152, 63
———. 2004b, ApJ, 606, 271
Hasinger, G., Schartel, N., & Komossa, S. 2002, ApJ, 573, L77
Helfer, T., & Blitz, L. 1997, ApJ, 478, 233
Ibata, R. A., Lewis, G. F., Irwin, M. J., Lehár, J., & Totten, E. J. 1999, AJ, 118, 1922
Irwin M. J., Ibata R. A., Lewis G. F., & Totten, E. J. 1998, ApJ, 505, 529
Ledoux, C., Theodore, B., Petitjean, P., Bremer, M. N., Lewis, G. F., Ibata, R. A., Irwin, M. J., & Totten, E. J. 1998, A&A, 339, L77
Lepp, S., & Dalgarno, A. 1996, A&A, 306, L21
Lewis, G. F., Carilli, C., Papadopoulos, P., & Ivison, R. J. 2002, MNRAS, 330, L15
Lewis, G. F., Chapman, S. C., Ibata, R. A., Irwin, M. J., & Totten, E. J. 1998, ApJ, 505, L1
Papadopoulos, P., Ivison, R. J., Carilli, C., & Lewis, G. 2001, Nature, 409, 58
Rowan-Robinson, M. 2000, MNRAS, 316, 885
Schöier, F. L., van der Tak, F. F. S., van Dishoek, E. F., & Black, J. H. 2005, A&A, 432, 369
Shalabiea, O. M., & Greenberg, J. M. 1996, A&A, 307, 52
Soifer, B. T., et al. 2004, ApJS, 154, 151
Solomon, P. M., Downes, D., & Radford, S. J. E. 1992a, ApJ, 387, L55
———. 1992b, ApJ, 398, L29
Solomon, P. M., Vanden Bout, P., Carilli, C., & Guelin, M. 2003, Nature, 426, 636
Sternberg, A., Genzel, R., & Tacconi, L. J. 1994, ApJ, 436, L131
Spergel, D. N., et al. 2003, ApJS, 148, 175
Usero, A., García-Burillo, S., Fuente, A., Martín-Pintado, J., & Rodríguez-Fernández, N. J. 2004, A&A, 419, 897
Vanden Bout, P. A., Solomon, P. M., & Maddalena, R. 2004, ApJ, 614, L97
Young, J. S., & Scoville, N. Z. 1991, ARA&A, 29, 581